DOI: 10.13009/EUCASS2023-462
Aerospace Europe Conference 2023 – 10TH EUCASS – 9TH CEAS

Transition of Pressure Oscillations in Hybrid Rocket Combustion using Paraffin Wax Fuel

Wonjeong Hyun[1], Sojung Park[2] and Changjin Lee†*
Konkuk University
Neungdongno 120, Gwangjin-gu, Seoul, 05029, Korea
gdw3433@konkuk.ac.kr –pistarty@hotmail.com
† cjlee@konkuk.ac.kr

Abstract
The post-chamber in hybrid rocket is a room for inducing an enthalpy increase, but it is related to triggering the mechanism leading to low-frequency combustion instability (<100Hz). Meanwhile, low frequency instability (LFI) is also commonly observed in paraffin wax combustion at the supercritical phase where the surface tension disappears. In this study, it was assumed that the LFI of paraffin wax combustion in the supercritical phase is also the result of mutual interference between turbulent flow and additional combustion. The present study aims to validate these assumptions by conducting a series of combustion tests and visualizing combustions in the post chamber.

1. Introduction

Hybrid rockets have the advantage of being able to control thrust, but their performance is low compared to other chemical rockets with higher specific impulse. The lower performance is due to the unburned fuel leaving the combustion chamber without an increase in enthalpy. The post chamber of a hybrid rocket engine (HRE) is an additional combustion volume that induces continuous combustion of unburned fuel [1] and is essentially important for improving combustion efficiency. A post chamber is also known to produce unwanted phenomena such as unsteady pressure oscillations and even low-frequency instability (LFI). Previous studies have shown that the periodic coupling of additional combustion in the post chamber and pressure disturbances due to vortex shedding is directly responsible for the occurrence of LFI [2]. Meanwhile, in the combustion of paraffin wax, a liquid layer melting on the fuel surface is usually formed, and entrainment of fuel droplets into the combustion gases is also observed. In addition, a molten liquid layer flows into the post chamber, where it interacts with the hot gases flow, generating additional fuel droplets [3]. A previous study showed that the unsteady pressure oscillations observed in the early stage of combustion are the result of additional combustion of fuel droplets of wax paraffin deposited in the post chamber [3].

Many studies have shown that LFI is a result of the resonance between the thermal lag characteristic of solid fuels and the oscillatory heat transfer to the solid fuels [4]. It is well known that the thermal lag frequency of solid fuels such as PMMA, HTPB, and paraffin wax is in the range of about 50Hz or less [5]. Also, several studies [6] reported that small vortices (in PMMA combustion) are the main cause of pressure oscillations in the 400-500 Hz band (p'), which are generated by the interaction of fuel evaporative flow with oxidizer flows on the surface. As unburned fuels trapped in small vortices are combusted in the post chamber, heat release fluctuations of the same frequency band (q') are also observed.

A recent study revealed that a positive coupling is periodically established between p' and q' while LFI is persisted [7]. This study attempts to investigate the detailed processes leading to periodic positive coupling (15-20 Hz) between p' and q' in PMMA combustion, where positive coupling was eventually identified as a substantial process to LFI. Another important physical process is the time evolution of the phase difference between the two oscillations. In a certain combustion environment, it is found that the phase difference changes periodically with time, resulting in pressure beats of about 15 to 20 Hz. At this time, the formation of 15~20 Hz pressure beats excite the oscillation of the boundary layer flow and the heat transfer oscillation on the fuel surface, which, in turn, could resonate with the thermal lag of the solid fuel developing into LFI. In addition, another interesting feature was found by analysing combustion images in post chamber. That is, it was observed that discontinuous flames accompanied by a slight ignition delay occur whenever pressure beats are formed, and that the ignition delay has a time-varying characteristic.

DOI: 10.13009/EUCASS2023-462

On the other hand, LFI was also observed in the combustion with paraffin wax fuel [8]. Note that since paraffin wax has a very low critical pressure, most of the combustion using paraffin wax takes place in supercritical phase. When combustion occurs in supercritical conditions, fuel droplet formation and entrainment may no longer be important physical phenomena to consider. Therefore, it is natural to assume that the combustion of paraffin wax in supercritical phase will have characteristics similar to PMMA combustion in which fuel droplets are hardly generated. It can also be assumed that the LFI of paraffin wax combustion is caused by the interaction of additional combustion and pressure disturbance in the post chamber, similar to that of PMMA combustion. As is known, the critical pressure and temperature of paraffin wax fuels depend on their carbon number. Reference [9] showed that the critical pressure and temperature of paraffin wax ($C_nH_{2(n+1)}$, n 20~40) are in the range of 5.8~11.5 bar (85 ~169 psi) and 680 to 860 K, respectively. And if *n* is in the median of 28-30, the critical pressure and temperature are 6.4 bar (94psi) and about 860K. Therefore, it is assumed that the LFI observed in paraffin combustion in supercritical phase undergoes a very similar physical process to that of PMMA combustion. In PMMA combustion, the LFI was found to be caused by the periodic coupling between unburned fuel combustion and pressure disturbance in post the chamber.

The purpose of this study is to verify the hypothesis by conducting a series of combustion tests. First, it is necessary to confirm that combustion with paraffin wax fuel is occurring in supercritical phase by measuring the combustion pressure and the temperature of the combustion gas and liquid layer in the post chamber, respectively. Additionally, combustion visualization of the post chamber will be attempted to capture the flame behavior and interaction with the gas flow impinging on the nozzle walls for test cases exhibiting LFI. It is also necessary to analyze the visualization data to check if ignition delay has occurred, which is a precursor of the LFI occurrence, as seen in PMMA combustion.

2. Combustion Test

2.1 Experimental set-up

Figure 1 shows a schematic of combustion chamber and test facilities. The combustion chamber consists of a 45 mm pre-chamber, 400 mm main chamber, a post chamber of 75mm and a nozzle. A quartz window was installed on the side of the post chamber to capture the images of flame behaviour and measure the heat-release fluctuations. Fuel is paraffin wax having an inner diameter of 18 mm and 400mm in length. Oxidizer is gaseous oxygen (GOx) was supplied through an axial injector and nitrogen gas was used to purge combustion gases after the tests. Oxidizer supply is controlled by MFC (mass flow controller). Pressure sensor (UNIK 5000 from General Electric) in the pre-chamber measures time traces of combustion pressure up to 1000 psi. Data sampling rate is 10,000 Hz. A band pass filter for 430 nm wavelengths was placed at the camera lens and PMT to clearly capture the heat release oscillations in terms of CH radicals. The light emission was measured by PMT (Photo Multiplier Tube, H10722 from Hamamatsu).

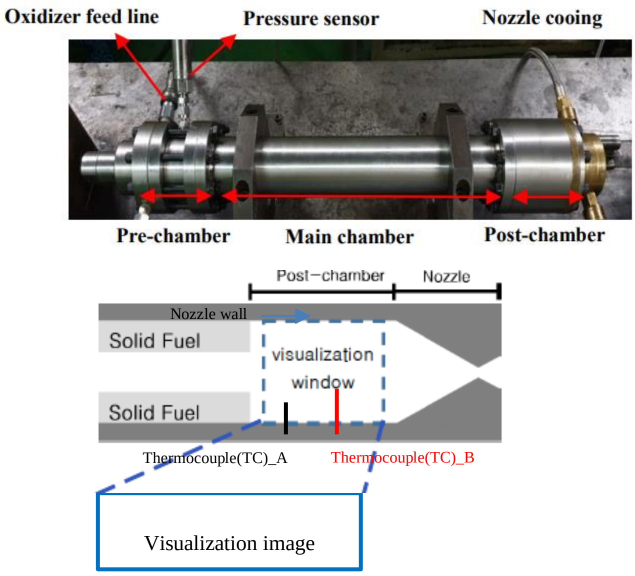

Figure 1: Configuration of the combustion chamber and sensor locations.

DOI: 10.13009/EUCASS2023-462

A high-speed camera (Casio Ex-1) was used to take a video footage of the combustion and gas flow in the post chamber. The camera was located 1 m away from the rear end of the nozzle. The frame rate of the camera is 1200 fps, which is fast enough to capture combustion pressure and heat release oscillations up to the 600Hz band. Thermocouples A(TC_A) and B(TC_B) are used for measuring the temperature of accumulated liquid layer and the combustion gas in the post chamber, respectively. Each thermocouple was located at distances of 25 mm and 50 mm from the rear end of the post chamber, respectively as shown in Fig.1. TC_A was radially protruded 5 mm while TC_B was inserted to protrude 12 mm from the post chamber wall. Data collection and process were done through DAQ boards and LabVIEW system.

2.2 Test set-up

Table 1 summarizes the various test condition. Four of these tests were conducted with transition from subcritical combustion to supercritical phase. Test 1 is the case with PMMA where the LFI was clearly observed, and is a reference case for comparison with the LFI in supercritical paraffin wax combustion (Test 4). Test 2 was done to compare the instability behaviors in paraffin wax combustion both in the subcritical and the supercritical phase. Both tests were done under the same test conditions. In test 2, combustion was maintained in the subcritical phase. Unsteady pressure oscillations were observed only at the beginning of combustion due to the droplets released from the liquid layer accumulated in the post chamber. In Test 3, the temperature of the liquid layer in the post-chamber was measured to determine whether the combustion takes place in the supercritical phase. The temperature measurements showed that the liquid layer in Test 3 was above the critical temperature.

Table 1: Summary of test conditions.

	Test 1	**Test 2**	**Test 3**	**Test 4**	**Test 5**
Fuel	PMMA	Paraffin	Paraffin	Paraffin	Paraffin
Inner diameter (mm)	20	18	18	18	18
Oxidizer mass flow rate (g/s)	20	20	50	80	80
O/F ratio	2.06	0.57	0.67	0.89	0.91
Post-chamber length (mm)	75	75	75	75	0
Remarks	[10]	Subcrit.	Supercrit.	Baseline	-

Test 4-5 were designed to sustain combustion in supercritical phase. Note that the stoichiometric ratio of paraffin wax/GOx combustion is 3.45. On the other hand, Test 4 is considered as a baseline test exhibiting well defined strong combustion instability, LFI. In this case, the flame in the post chamber was also visualized. Results in test 4 were compared with those of Test 1 both in spectral analysis of combustion pressure and flame images at the instability. Also, Test 5 was conducted without post chamber to understand the role of post chamber in triggering the LFI. It is worth to note that combustion pressure was maintained approximately 200 psi in every test by changing nozzle throat for safety reason. The diameters of each nozzle throat are Test 1-2: 6 mm, Test 3-4: 8 mm, Test 5: 10 mm.

3. Results and discussion

3.1 Paraffin wax combustion in supercritical phase

Supercritical fluids refer to a substance at a temperature and pressure above critical values. They exhibit moderate physical properties between gas and liquid phase and have good diffusion force because no surface tension exists. As a consequence, the transition of liquid layer in the post chamber to the supercritical phase prevents droplet formation due to the lack of surface tension. Instead, turbulent mixing of gasified fuel flow rather than droplet formation appears

DOI: 10.13009/EUCASS2023-462

to be the dominant phenomenon [9]. Because of the supercritical environment, it can be assumed that the paraffin wax combustion will exhibit very similar characteristics to that of PMMA already investigated in previous study [10].

Therefore, LFI in paraffin wax combustion is expected to occur through a mechanism very similar to that of PMMA combustion, a polymer-based fuel without a liquefaction process. In order to verify this hypothesis, it is important to first confirm that the paraffin wax liquid layer accumulated in the post chamber is in a supercritical condition. To this end, the temperature of liquid layer in the post chamber and combustion pressure need to be measured respectively and compared with supercritical conditions of paraffin wax combustion.

3.1.1 Liquid layer temperature

Thermocouples A (TC_A) and B (TC_B) are located to measure the temperature of the liquid layer and combustion gas in the post chamber, respectively, as shown in Fig. 1. TC_A is located to measure the temperature of the liquid layer surface. For that, the accumulated thickness of the liquid layer was measured in advance, and found to be approximately 5 mm.

Figure 2 shows the liquid layer accumulated after combustion and thermocouples for temperature measurements during the combustion test. In Fig. 2a, the probe TC_A was almost submerged in the liquid layer, and only the convex silhouette of the thermocouple was observed. The probe TC_B protruded above the liquid layer, thereby confirming that the temperature of the combustion gas in the post chamber was properly measured.

Figure 3 shows time trajectories of the combustion pressure and temperature of liquid layer in Test 3. Both pressure and temperature data were collected simultaneously through the DAQ board. In Fig. 3b, TC_A measurement, the temperature reached 680K at about 0.8 sec and maintained approximately 827K for about one second. As mentioned, the critical temperature of the paraffin wax ($C_nH_{2(n+1)}$, n=20~40) is in the range od 680~860k and is approximately 860K when n=28~30. And TC_A temperature measurement confirmed that liquid layer reached a critical temperature or higher within just one second after ignition. Note that the response delay of thermocouple is about 0.05 sec. In the TC_B measurement, the temperature of combustion gas increased and maintained its maximum for about one second, then gradually decreased until nitrogen gas was introduced for purging. It is interesting to note that LFI in paraffin wax combustion is observed after reaching the supercritical temperature, especially in conjunction with the combustion pressure trajectory.

In addition, since Test 2-5 were conducted under the fuel-rich conditions, we expect the combustion temperature to increase as the O/F ratio increases (Table 1), and accordingly, the liquid-layer temperature in Test 4-5 would be above the critical temperature. Therefore, the next section will be devoted to observing some physical parameters with increasing paraffin wax combustion pressure and temperature and determining that the combustion condition has attained the supercritical phase.

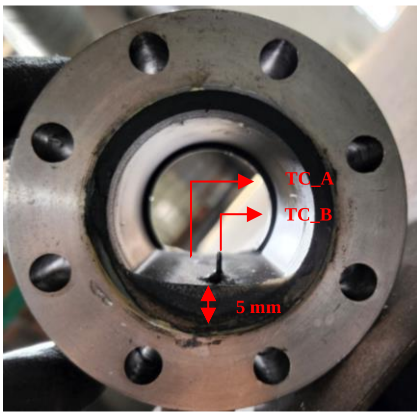

Figure 2: Thermocouple TC_A and TC_B, and accumulated liquid layer after a test.

DOI: 10.13009/EUCASS2023-462

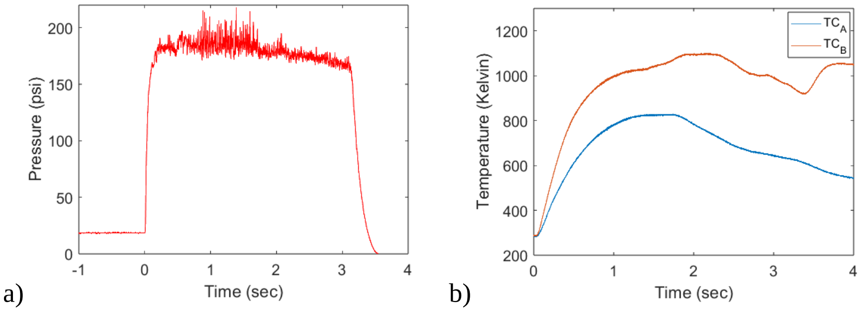

Figure 3: a) Trajectory of the combustion pressure and b) temperature of liquid layer in Test 3.

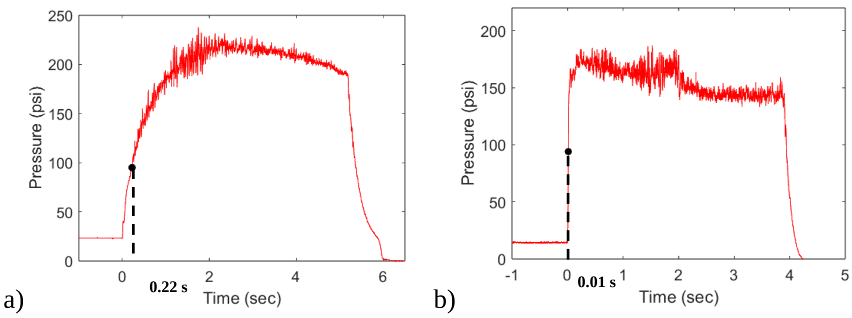

Figure 4: Comparison of pressure trajectories and critical points in a) Test 2, b) Test 4

3.1.2 Streak-lines with increasing combustion pressure

In addition to the liquid layer temperature measurement, an interesting fact can be found by comparing the change of the streak lines at the rear end of the nozzle in Test 2 (low O/F ratio) and Test 4 (high O/F ratio). As mentioned, the critical pressure of paraffin wax ($C_nH_{2(n+1)}$, n 20~40) is about 94 psi when n is in the range of 28~30. Figure 4 compares the time trajectories of combustion pressure in Tests 2 and 4, respectively, and the black dot is the point where the critical pressure (94psi) has been reached. As shown, it takes 0.22 sec (Test 2) and 0.01 sec (Test 4) respectively to reach the critical pressure.

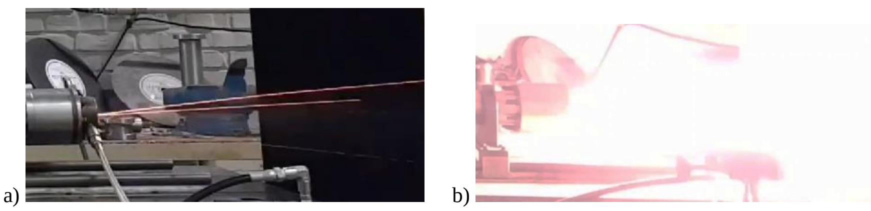

Figure 5: Comparison of combustion images at the rear end of the nozzle in a) Test 2 and b) Test 4.

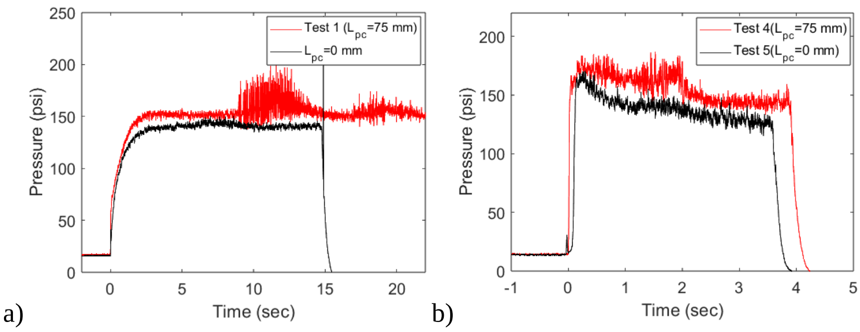

Figure 6: Comparison of pressure trajectories with and without post chamber for
a) PMMA/GOx [11], b) paraffin wax/GOx (Test 5)

DOI: 10.13009/EUCASS2023-462

Figure 5 compares raw images of flame at the rear end of the nozzle at 0.1 sec after ignition in Test 2 and Test 4. At this point, Test 2 was in the subcritical phase even it reached a critical pressure because its temperature was under the critical one, and Test 4 seems to be in the supercritical phase after reaching critical pressure. Fig. 5a showed raw images of flame after the nozzle containing streak-lines of unburned particles. This is one of the physical evidences that droplets are formed and burned in the subcritical pressure regime [9]. On the other hand, Test 4 is thought to have reached the critical pressure within a very short time, and in this case, no streaks are observed in the wake flame. Combining these physical observations and temperature measurements of the liquid layer, it was confirmed that the supercritical combustion conditions were maintained in Tests 3, 4, and 5.

3.2 Combustion pressure

3.2.1 With and w/o post chamber

In the previous section, it was assumed that the combustion characteristics of paraffin in the supercritical phase would be similar to that of PMMA. The most interesting feature is that the combustion became perfectly stable when the post chamber was removed. Therefore, installation of the post chamber and additional combustion are considered to be prerequisites for determining the LFI occurrence. In order to verify the hypothesis, Test 5 was conducted without post chamber while other parameters fixed.

Figure 6 compares the pressure trajectories with and without post chamber in hybrid rockets using PMMA/GOx [11], and paraffin wax/GOx, respectively. The test conditions for each solid fuel were unchanged in both cases. As shown in the figure, unstable pressure oscillations and/or LFI are only observed for test cases with a post chamber. Therefore, it can be assumed that the post chamber can be a source of unwanted side effects such as unstable oscillations and combustion instability. In this regard, even in paraffin wax combustion, LFI occurrence is presumed to be caused by certain physical processes associated with additional combustion in the post chamber. To verify this assumption, in the next section, the combustion pressure in PMMA combustion (Test 1) and in paraffin wax combustion (Test 2, Test 4) will be compared and analyzed. This investigation is expected to provide more conclusive evidence to determine whether the combustion of paraffin wax in supercritical phase is very similar to that of PMMA.

3.2.2 Conditions for LFI occurrence: PMMA vs. Paraffin wax

Previous studies [10, 11] reported there are several specific conditions for the LFI occurrence in PMMA/GOx system. Here are the details of specific conditions.

① Amplification of p' $and\ q'$

High-frequency oscillations (p' and q') in frequency band of 400 to 500 Hz are observed due to the interaction between the fuel evaporation flow and the oxidizer flow.

② Periodic formation of positive coupling between $p'\ and\ q'$

During the LFI, the phase difference between p' and q' changes periodically with time, resulting in periodic positive coupling between p' and q'. And this causes pressure beats with a frequency very similar to the thermal lag of solid fuels.

③ Re-ignitions with delays in the post chamber

In a previous study, it was observed that additional combustion in the post chamber was accompanied by an ignition delay, and the phase difference between p' and q' was affected by the change in the magnitude of the ignition delay. That is, the ignition delay is involved in the periodic coupling of p' and q', leading to the generation of pressure beats, which ultimately acts as an external perturbation to the boundary layer.

In this regard, this section aims to confirm whether the three conditions (①-③) directly related to the occurrence of LFI also would appear in Paraffin wax/GOx combustion whenever LFI occurs.

DOI: 10.13009/EUCASS2023-462

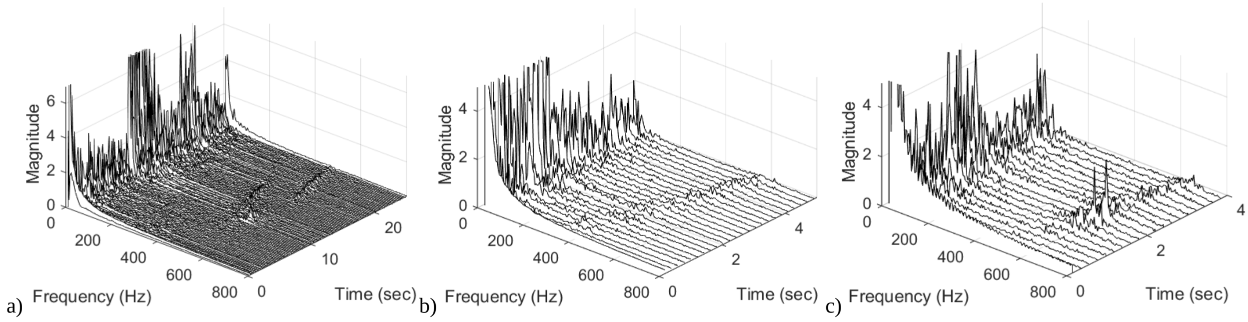

Figure 7: Spectral analysis of the combustion pressure in a) Test 1, b) Test 2, c) Test 4

Figure 7 shows spectral analysis of the combustion pressure in Test 1, Test 2, and Test 4, respectively. In Fig. 7a (Test 1, PMMA/GOx combustion), LFI in the 15-20Hz band was observed between 9 and 13 s. The high-frequency characteristics in the 400–500 Hz band (p′) were suddenly and simultaneously amplified at the point of LFI. In addition, the frequency band of p' over time gradually decreased followed by the frequency jump. In Fig. 7b (Test 2, subcritical phase paraffin wax/GOx), a strong unsteady pressure oscillation occurred in the 30Hz band only at the beginning of the combustion. High-frequency component of the combustion pressure was also amplified very weakly throughout the combustion. The frequency band was shifted from 400Hz to 600Hz in this case, which was not observed in PMMA combustion.
In Fig 7c, (Test 4, supercritical phase paraffin wax/GOx), Low frequency combustion instability of the 30-50Hz band was suddenly initiated during the combustion, while a high-frequency component in the 600Hz band (p') was also amplified simultaneously. Spectral analysis in Test 4 appears to be very similar to the occurrence of LFI observed in Test 1, although the peak frequency bands do not match. Another interesting feature in Test 4 is that the high-frequency band of p' gradually increases, while in Test 1 the high-frequency band of p' decreases with time. Comparing the two results, even in the combustion of paraffin wax in supercritical phase, the formation of p' is an important factor that significantly affects the generation of LFI, and it has the same characteristics as the ①-condition described in the previous section. However, the formation of positive coupling of the two oscillations was not directly confirmed because the measurement of q' synchronized with p' was not made in Test 4.

3.3 Visualizing combustion in post chamber

In order to see whether the conditions of ② and ③ appear even in supercritical paraffin wax combustion, it is necessary to measure heat release oscillation (q′) in the post combustion chamber due to additional combustion. Two different methods are available for measuring q' in the post chamber. The first method is to take flame images in the post chamber through CH* filter attached to the quartz window. Since CH* radical, one of the short-lived chemical species, emits light at a certain wavelength during the combustion process, the intensity of CH* radical chemiluminescence is a good marker of heat release. And it is well known that CH* radicals are produced spatially near the region of the first sharp temperature rise in the reaction zone, creating an outline of blue/violet photons [12-13]. Therefore, it can be analyzed intensity measurement of CH* radials approximate local heat release, and has the advantage to accurately monitor temporal change in additional combustion in the post chamber.

However, in practice, since combustion soots are easily deposited onto the window and the amount of incoming light into the camera constantly decreases, it is difficult to measure the emission intensity of CH*. Another alternative is to take only the light intensity emitted from combustion in the post chamber without the using a filter. This method cannot accurately measure the heat release oscillation because it cannot accurately capture the combustion area, but it can simply estimate the heat release oscillation from measuring the change in intensity of the flame image. In addition, even if soot is deposited to the visualization window, this method has an advantage that quantitative information can be obtained on the heat release oscillation. In paraffin wax combustion, the visibility of the visualization window is greatly reduced due to the liquid layer and droplets contained in the combustion gas. Therefore, in this study, the second method was adopted as the alternative choice for heat release measurement.

DOI: 10.13009/EUCASS2023-462

3.3.1 Visualization in post chamber

Since paraffin wax combustion in supercritical phase produces too much soot deposition on the visualization window, heat release oscillation (q') was approximated by luminosity variation from flame images through the quartz window. To obtain the luminosity data, it is necessary to extract light intensity from the images. Here is the brief of how data image was processed. High speed images are recorded as a .mov format file. Firstly, the movie is decompressed for each frame, and is converted to YUV file. This process is done by a software called "fftmpeg", in-house code. The representative luminosity for each frame is computed by summing all the brightness data from each pixel within the frame. Then, the change in the total amount of light over the entire combustion time can be identified, and q' was approximated by the temporal change of luminosity. This data could be used for spectral analysis of q'.
Note that flame images for Test 1 were taken between 10 and 13 sec, where the LFI is evident. In Test 4, combustion images were captured from 1.5 to 2 sec.

3.3.2 Combustion in post chamber: PMMA vs. Paraffin wax in Supercritical Phase

Figure 8 shows a collection of flame images of additional combustion taken in the post chamber during which the LFI appears in Test 1. Reference [10] addresses the details of evolution of flame and the existence of ignition delay. The flow boundary is marked with a red line to encircle the flow regions that contain unburned fuel mixture. The white area is a high-temperature flame in the post chamber. After the flame extinguishes (Fig. 8a), the flow region extends toward the nozzle wall, and the jet-shaped flow collides with the nozzle wall (Figs. 8b and 8c). Upon collision, a large vortex-shaped flow bounces back into the upstream of the post chamber (Figs. 8d and 8e). As the bounced-back flow collides with the incoming flow, the flow containing unburned fuel mixture expands throughout the chamber volume (Fig. 8f), and re-ignition occurs (Fig. 8f). The re-ignited flame expands and completely consumes the unburned fuel. A cyclic behavior is then observed (Fig. 8h → a) after complete burning (Fig 8h). Here, the ignition delay is the delay time from when the flow collides with the wall until ignition occurs again (Figs. 8c and 8e). This cycle was observed to form repeatedly at about 15 times/s, that is nearly identical to the LFI frequency band observed in PMMA. As a result, it can be though that the formation of counterflow and the ignition delay of unburned fuel in the post chamber are closely correlated with the onset of the LFI.

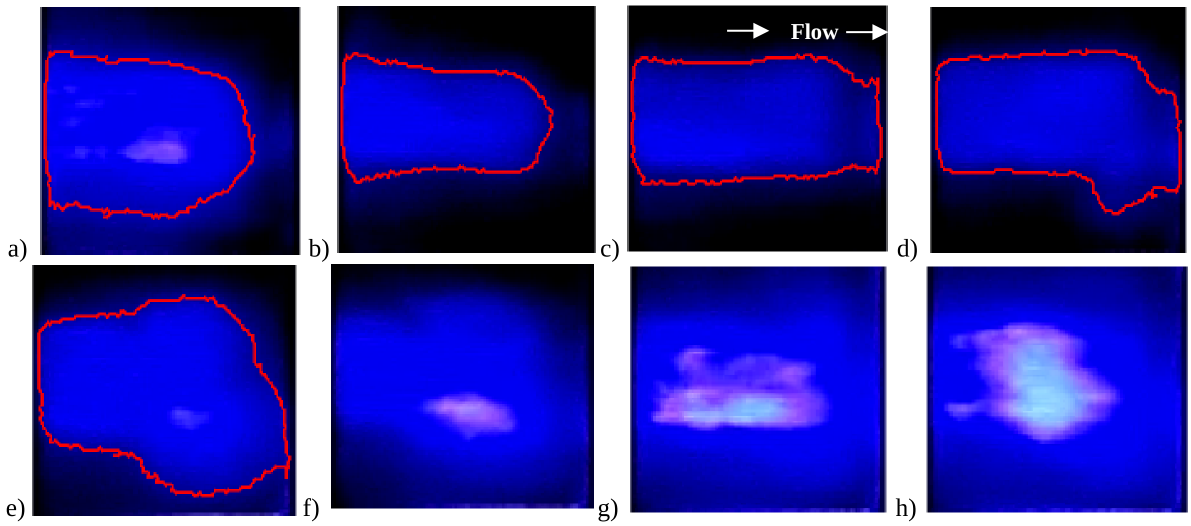

Figure 8: Sequential images of the additional combustion in the post chamber within one cycle in Test 1 [10].

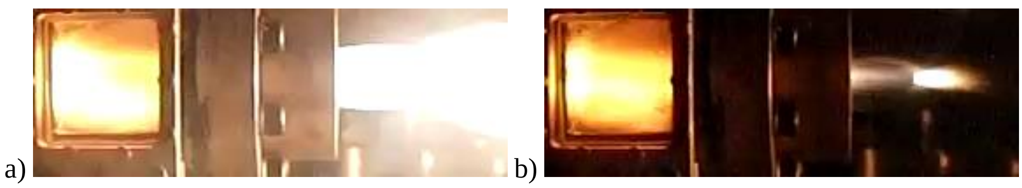

DOI: 10.13009/EUCASS2023-462

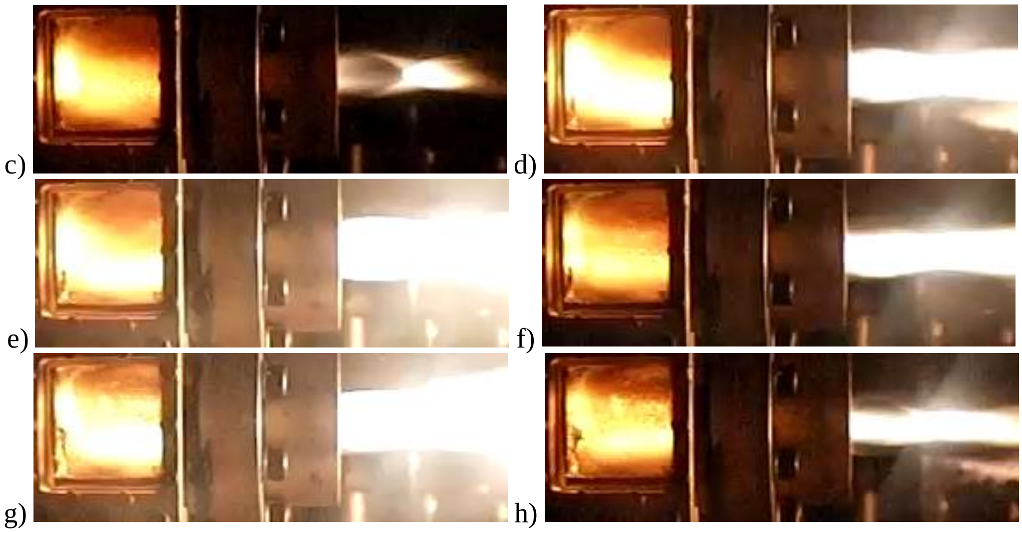

Figure 9: Sequential images of the additional combustion in the post chamber in Test 4

Figure 9 shows the visualized image taken between 1.8 and 2.5 seconds in which LFI appears in Test 4. The time interval of each image is 0.85 sec. The flame is represented as a bright orange area due to the absence of a CH* filter. Although a precise analysis of the flow in the post-chamber was unattainable, the re-ignition (Fig. 9a, 9d, 9e, 9g) and extinguishment (Fig. 9b, 9c, 9f, 9h) of the flame were observed. In addition, the flame was mainly located near the left side of the post chamber. This is very similar to the flame locations seen in Fig. 8 and satisfies the ③ condition summarized in the previous section. To obtain more detailed information, luminosity measurement was attempted along with visualization.

Spectral analysis for luminosity variation of Test 1 and Test 4 are compared in Figure 10. High-frequency component of luminance in the 400–500 Hz band (q') was suddenly amplified as the LFI began in Test 1. Similar to the previous case, in Test 4, q' was amplified in the 600Hz band and the luminosity in the low frequency band was also amplified. Interestingly, in paraffin combustion as in PMMA combustion, the frequency band of q′ consists of two separate bands, a low frequency and a relatively high frequency, just like the two frequency bands of p′ shown in Fig. 7c. Although the approximation of q' by flame luminosity measurement cannot accurately determine the coupling status between p' and q', if q' could be measured in more accurate way, the periodic change in coupling status between p' and q' would be possible.

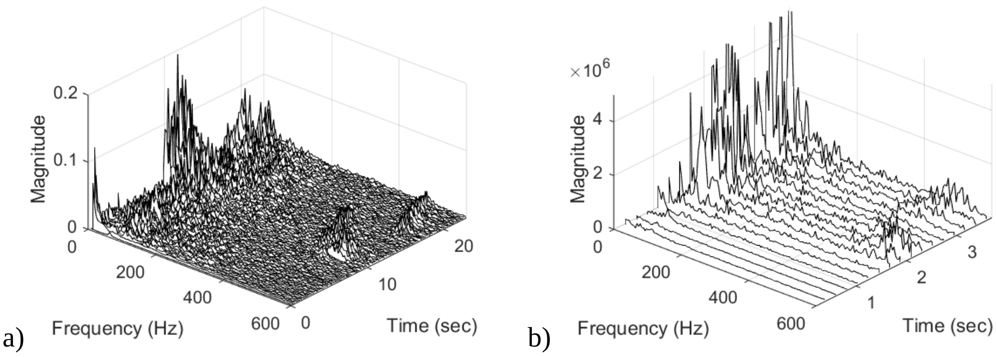

Fig. 10. Spectral analysis of luminosity variation in a) Test 1(PMMA) and b) Test 4(Paraffin)

3. Conclusion

The LFI in paraffin combustion in supercritical phase was hypothesized to be caused by the periodic coupling of unburned fuel combustion and pressure disturbance in the post chamber, and this interaction is very similar to the physical processes observed in the LFI occurrence in PMMA combustion. The purpose of this study is to verify this

DOI: 10.13009/EUCASS2023-462

hypothesis by conducting a series of combustion test with paraffin wax fuel, and also to visualize the post chamber flow and flame behaviors.

In paraffin wax combustion in supercritical phase, it can be assumed that the LFI, since the surface tension of the liquid disappears and no droplets are generated, can be occurred in a way similar to the LFI occurrence in the PMMA combustion [11]. In order to investigate that combustion condition of paraffin wax combustion, the temperature of the liquid layer accumulated at the bottom of the post chamber was measured. In Test 3, the temperature of liquid layer reached 800K, which was higher than the supercritical temperature of 680K, confirming that combustion was occurred in a supercritical phase.

Combustion condition can be qualitatively determined by streak-lines of unburned fuel droplets that appears downstream of the nozzle. In Test 2, streak-lines by unburned fuel droplets were clearly observed for 0.5 sec before the combustion pressure reached the supercritical phase. However, in Test 4, since the supercritical pressure was almost instantly attained, streak-lines were not observed at all. This is another evidence that paraffin wax combustion was in the supercritical phase without droplet formation. And combustion characteristics similar to those observed in PMMA combustion (Test 1) are expected to dominate, and the occurrence of LFI is expected to occur by the same mechanism.

By examining the basic conditions for LFI occurrence confirmed in PMMA combustion, it is possible to qualitatively determine whether the same LFI process can be applied to supercritical paraffin combustion of paraffin where no liquid droplets are formed. First of all, the LFI did not occur in any case without post chamber. As another notable similarity, the occurrence of pressure disturbance (p') in the 500Hz band was observed simultaneously with the occurrence of LFI. In addition, heat release fluctuations (q') in the same frequency band were also measured by post chamber visualization. Finally, during LFI occurrence, discontinuous flame behaviors are exhibited, similar to that observed in previous studies on PMMA. These similarities provide strong evidence that the occurrence of p' and q' and their periodic coupling are the decisive processes leading to the LFI occurrence in paraffin wax combustion. However, due to the soot deposition, the visualization method could not provide an accurate change in q' and could not confirm the dynamic change and their coupling of p' and q'. Therefore, in future studies, it is necessary to comprehend how q' occurs in paraffin wax combustion and accurately measure the dynamic change in coupling status between p' and q'.

Acknowledgments

This work was supported by the National Research Foundation of Korea (NRF) grant by the Korea government (MSIT) (No. 2021R1F1A1061516132068207325010З).

References

[1] Messineo, J., Lestrade, J.Y., Hijlkema, J., Anthoine,J.: Vortex shedding influence on hybrid rocket pressure oscillations and combustion efficiency, *J. Propuls. Power* 32(6): 1386–1394.

[2] Moon,Y.J., Lee, C.J.: Dynamics of Post Chamber Flame and Combustion Pressure in Hybrid Rocket, *52nd AIAA Joint Propulsion Conference*.

[3] Hyun, W. J., Lee, C. J.: Unsteady Pressure Oscillations of Liquefied Paraffin Wax Combustion in Hybrid Rocket, *J. Korean Soc. Aeronaut. Space Sci.* 50(5): 339-347.

[4] Karabeyoglu, A., Zilwa, S.D., Cantwell, B., Zilliac, G.: Modeling of hybrid rocket low frequency instabilities, *J. Propuls. Power*, 21(6): 1107–1116.

[5] Karabeyoglu, A.: Thermal Transients in the Hybrid Rocket Fuel Grains - Nonlinear Effects, *43rd AIAA Joint Propulsion Conference & Exhibit, Cincinnati*.

[6] Kim, D.Y., Lee, C.J.: Destabilization of the Shear Layer in the Post chamber of a Hybrid Rocket, *J. Mech. Sci. and Technol.*, 30(4): 1671–1679.

[7] Hyun, W. J. Lee, C. J.: Thermoacoustic Coupling Depending on Post-chamber Configuration in Hybrid Rocket, *Proceeding of 8th edition of the space propulsion conference*, SP2022_75.

[8] Zilliac, S. D., Karabeyoglu, A., Zilwa, G., King, L., Reinath, M.: Combustion Oscillations in High Regression Rate Hybrid Rockets, *Proceeding of 39th AIAA Joint Propulsion Conference and Exhibit*, AIAA Paper 2003-4465.

DOI: 10.13009/EUCASS2023-462

[9] Leccese, G., Bianchi, D., Nasuti, F.: Modeling and Simulation of Paraffin–Based Hybrid Rocket Internal Ballistics, *2018 Joint Propulsion Conference*.
[10] Hyun, W. J., Lee, C. J.: Modeling for Thermoacoustic Instability and Beating Pressure Amplification, *J. Korean Soc. Aeronaut. Space Sci.* 50(11): 783-789.
[11] Hyun,W. J., Kim, J. A., Chae, H. S., Lee, C. J.: Passive Control of Low-Frequency Instability in Hybrid Rocket Combustion, *Aerospace*, 8(8): 204.
[12] Hardalupas, Y., Orain, M.: Local measurements of the time-dependent heat release rate and equivalence ratio using chemiluminescent emission from a flame, *Combustion and Flame* 139: 188-207.
[13] Karnani, S., Rankin, D. D.: Visualizing CH chemiluminescence in sooting flames, *Combustion and Flame* 160: 2275-2278.`